DETERMINATION OF THE MICROSTRUCTURAL EVOLUTION DURING THE BATCH ANNEALING OF MICROALLOYED STEEL COILS[1]

Oswaldo L.G. Branchini [2]
Antonio Augusto Gorni [3]
André Paulo Tschiptschin [4]

ABSTRACT

The aim of this work was the determination of microstructural evolution of a cold rolled Nb microalloyed steel sheet submitted to a thermal cycle comprised of slow heating up to a temperature of 670°C followed by a soaking treatment of ten hours under this temperature. This treatment was basically a physical simulation of the industrial steel coil batch annealing process. It was performed in a muffle furnace using the same sequence of time, temperature and heating rates observed at an industrial plant. During this simulated treatment samples were took off from the furnace at pre-determined times and temperatures. These samples were submitted to quantitative metallographical analysis and to hardness testing. This information allowed the identification and analysis of the metallurgical restoration mechanisms operating during the annealing process.

[1] *Paper presented at the 2nd International Conference on HSLA Steels, Chinese Society for Metals, Beijing, October 28-November 2, 1990.*

[2] *Development Engineer, COSIPA Steelworks, Cubatão SP, Brazil.*

[3] *Research Engineer, M.Eng., COSIPA Steelworks, Cubatão SP, Brazil,*

[4] *Professor, Ph.D., M.Sc., Polytechnical School of the São Paulo University, São Paulo SP, Brazil.*

- INTRODUCTION

The determination of the microstructural evolution of coiled cold-rolled sheet during batch annealing can provide vital data to a correct specification of the industrial process, which can allow the reduction of its cost and assuring good quality and consistent properties in the final product [1]. Such study, however, must take place under laboratory scale, to guarantee the precision of the treatment parameters and to avoid the considerable disturbance that would occur if the trials were developed at the plant [2].

The annealing of microalloyed steels has some particular aspects, as niobium alters austenite and ferrite restoration processes. This element retards steel recovery and recrystallization, increasing incubation time necessary for nucleation of the ferrite grains, as well their growing rate. This element retards recrystallization either in solid solution ou in precipitated form.

When Nb amount exceeds the stoichiometric ratio it can stabilize the subgrain boundaries through the formation of clusters, so they hardly move. This fact leads to an increase in the minimum temperature necessary for the recrystallization start in relation to a mild steel. This increase is proportional to the amount of Nb.

The effect of Nb as precipitates – carbides and/or carbonitrides – will depend upon their size and distribution. Eventually unexpected effects can occur, as the niobium carbonitrides can be partially coherent with the ferritic matrix. This facilitates an intense nucleation of fine dispersed carbonitrides, which can cause an increase in mechanical strength and in crystallographical texture of the structure after cold rolling and recrystallization [3-8].

Great second phase particles, with size about 400 angstroms, promote an acceleration of recrystallization as their great hardness increases the local density of dislocations after cold rolling, which facilitates the nucleation of recrystallized grains on its interface.

Recrystallization takes place through nucleation and growth mechanisms. Factors that contribute to increase the nucleation rate lead to a more refined ferritic grain after recrystallization. If recrystallization kinetics is enhanced by the existence of particles in the microstructure matrix, a significantly refined ferritic microstructure is got after recrystallization, with an average grain diameter of 5 μm.

On the other hand, if precipitates are very finely dispersed, recrystallization is delayed due to the inhibition of the nucleation of new grains. In this case the number of active nuclei available for recrystallization decreases and final ferritic grain size increases.

The growth process of the recrystallized grains can be classified in two categories, according to the microstructure where the grain is growing: a) a deformed or recovered matrix, or b) an already recrystallized matrix.

Another important fact that can affect recrystallization kinetics is the coiling temperature after the hot strip rolling process. In the case of steels with a very high Nb amount (greater than 0.109%), the coiling between 650 and 550°C exerts little influence. However, for lower amounts of Nb (less than 0.085% and with a Nb/(C+N) ratio equal to 7.0), the steel coiled at 550°C can recrystallize under a lower temperature. In this case some amount of C and N can be still in solution, and so they can form precipitates during the recrystallization treatment, promoting nucleation and supressing the growth of recrystallized grains [5].

The microstructures observed for these two coiling temperature conditions are totally different. Steels with more than 0.030% Nb and coiled at 550°C show equiaxial recrystallized grains and lower plastic anisotropy; however, coiling at 650°C led to a microstructure with elongated grains and greater plastic anisotropy [4,8,9].

Another factor that affects the recrystallization kinetics is the heating rate. An increase in the heating rate shifts the temperature of recrystallization start to higher values, irrespective of the Nb amount (0,034 ~ 0,320%) and coiling temperature (650 ~ 550°C) [5].

- EXPERIMENTAL PROCEDURE

The steel selected for this study had the following composition: 0.070% C, 0.65% Mn, 0.044% Nb, 0.079% N, 0.058% Al_{tot} and 0.010% S. This product is normally used for the manufacture of deep-drawed automotive parts. During its processing at the Hot Strip Mill the finishing and coiling temperatures applied were equal to 870±20°C and 600±20°C, respectively. The samples for the laboratory simulated annealing were got just after strip processing at the cold tandem mill. The as-cold rolled sample reserved for the characterization of the cold work structure was designated as **LTF**. Additional samples of this material were got after hot strip rolling and industrial batch annealing; they were designated as **LTQ** and **REC**, respectively.

The samples collected at the cold tandem mill were submitted to the simulated annealing treatment in a laboratory muffle furnace. This heat treatment was quite similar to the industrial box annealing process applied at COSIPA. The temperature evolution in the laboratory muffle furnace followed the same values of time, temperature and heating rates observed at the plant. The real temperature-time annealing cycle used at the plant was divided into nine linear segments in order to simulate the coil batch annealing process.

The control and monitoring of the muffle furnace were performed by a digitally programmed control device coupled to an IBM-XT microcomputer. A BASIC program was used to control the furnace temperature, using as input variable the moving average of the last eight measured temperatures; this routine also saved temperature and time data in floppy disks during all treatment, thus assuring the complete recording of the heat treatment parameters. The electric system was fully grounded, including the thermocouple sheaths, in order to avoid interference and noise disturbances in the signals generated by the chromel-alumel thermocouples. Two

temperatures were recorded: in the furnace chamber and in the metallic box that contained the samples.

The simulation was performed at the laboratories of the Department of Metallurgical Engineering at the Polytechnical School, São Paulo University. The samples were previously blast cleaned with steel shot and put in a stainless steel box full of steel shot which was introduced in the muffle furnace. Pure nitrogen was injected in the furnace chamber in order to avoid the oxidation of the samples, in the same way it is done during the industrial box annealing process.

During the annealing cycle 27 samples were periodically taken out and water quenched according to a previously established time-table; they were designated with letters, from **A** to **Z**, plus **AA**. The scheduled time-temperatures for sample withdrawal can be seen at table I. One additional sample, designated as **ZA**, was cooled inside the furnace.

A greater number of samples was taken out in three specific temperature ranges where the activation of the main metallurgical restoration mechanisms was to be expected. The first special temperature range varied from 150 to 400°C; it was chosen because the recovery processes start at these temperatures. Six samples (**B** to **G**) were taken out between the four hour heating between these two temperatures. The second selected temperature range varied from 480 to 580°C, when six samples (**I** to **N**) were taken out; it is believed that in this specific stage of the thermal cycle the recovery processes are dominant and, eventually, there is some recrystallization. The last selected temperature range varied between 630 and 670°C, corresponding to the full recrystallization region; the heating of the samples between these two limits took seven hours. Four samples (**S** to **V**) were extracted during this time span. All samples took off during these special temperature ranges were submitted to a detailed microstructural analysis using optical microscopy in order to study the restoration phenomena involved.

The remaining samples were used to check the microstructural evolution along the whole heat treatment, specially regarding the soaking

period (670°C during 10 hours). Five samples were taken out during this period (**V** to **Z**). A furnace cooled sample (**ZA**) served to establish a comparison between the microstructure got after the simulated laboratory annealing and the microstructures observed in the industrial coils annealed at the plant.

Sample	Aimed Extraction Temperature [°C]	Real Extraction Temperature [°C]	Extraction Time [hour:min]	Temperature Difference (Aimed-Real) [°C]	Hardness [HV 500g]
A	100	84	00:15	16	280
B	174	152	00:30	22	281
C	224	213	00:40	11	292
D	276	273	01:00	3	295
E	303	302	01:15	1	293
F	386	372	02:45	14	303
G	408	399	03:15	9	291
H	440	439	05:15	1	290
I	476	470	08:15	6	286
J	506	499	09:00	7	282
K	533	526	10:00	7	295
L	550	559	11:00	-9	297
M	558	549	12:00	9	271
AA	569	580	13:30	-11	285
N	583	588	15:15	-5	278
O	590	587	16:15	3	254
P	598	606	17:15	-8	263
Q	609	612	18:45	-3	203
R	618	620	20:15	-2	196
S	629	626	21:45	3	176
T	640	642	23:15	-2	168
U	653	657	25:15	-4	175
V	668	672	27:30	-4	173
W	670	676	30:00	-6	162
X	670	676	32:30	-6	158
Y	670	675	35:00	-5	162
Z	670	665	40:00	5	160
ZA	20	20	48:00	0	141

Table I: Scheduled and real temperatures/times for withdrawal of samples from the muffle furnace and their corresponding hardnesses.

The metallographical technique used for microstructure revelation using optical microscopy consisted of sample grinding with silicon carbide paper, 180 through 600 grit, and polishing on a fine canvas cloth impregnated with 6-μm diamond compound, using ethyl alcohol as lubricant. This step was repeated using fine diamond paste of 3 and 1 μm.

Finally, the polished samples were etched with Nital 3% for the observation of the ferritic grain boundaries.

The determination of ferritic grain size was made through the observation of the samples using a glass disk inserted in the microscope eyepiece. The number of intersections of the ferritic grain boundaries with a 25132,7 μm long test line was counted under a magnification of 800 times [10,11]. The recrystallized fraction was determined using an 169 point grid [10,12]. The hardness of the samples was determined in the same polished and etched surfaces prepared for metallographic analysis using a Vickers testing machine with a 500 g load [10,13]. For each sample the number of observations of the ferritic grain sizes, recrystallized fractions and Vickers hardnesses was chosen in order to guarantee a maximum mean error of 5% considering a 95% statistical confidence level.

The identification of the niobium precipitates required the isothermal annealing of a sample at 630°C for 10 hours in order to promote their growth. Then this sample was submitted to selective dissolution in a 20% HCl solution which was subsequently filtered. The extracted precipitates were then identified through X-ray diffraction [10].

Transmission electronic microscopy was used to check the recovery and recrystallization processes start in the samples during the simulated annealing cycle. The samples selected for this analysis were **LTF**, **F**, **P**, **Q** and **ZA**.

- RESULTS

Samples of the material as hot strip (**LTQ**), cold strip (**LTF**) and batch annealed coil (**REC**) were characterized in terms of their ferritic grain size and hardness. This data will be used later as reference parameters for the initial and final stages of the physical simulation of the batch annealing treatment. These results can be seen at table II.

Table III shows the results of the mean value statistical analysis performed with the difference between real and aimed temperatures at the moment of sample withdrawal which are listed in table I. Figure 1 shows graphically the programmed and real annealing temperature cycle, as well the differences observed between their aimed and real values, while figure 2 shows the evolution of sample hardness along treatment time.

	Grain Size [μm]	**Hardness [HV 500 g]**
LTQ	5.6	175
LTF	2.0	264
REC	5.2	134

Table II: Microstructural parameters of the hot and cold coils processed at COSIPA plant.

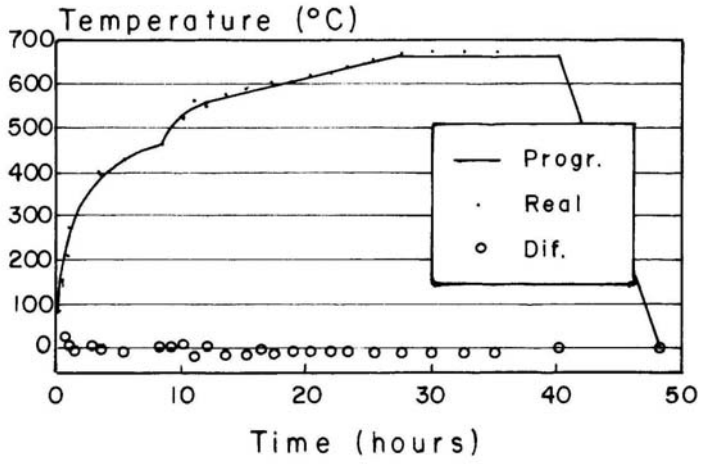

Figure 1: Programmed and real simulated annealing temperature cycle, including temperature deviations observed along treatment time.

The samples were divided in two groups for the purposes of microstructural analysis: a) samples that were submitted to the recrystallization process, **O** through **U**; b) samples which showed grain growth after full recrystallization, **T** through **ZA**. Table IV and figures 3 and 4 show the evolution of recrystallized fraction and grain size along annealing cycle time. In these graphics the instant zero corresponds to the start of the considered phenomenon, and not the time after the beginning of the simulated annealing cycle.

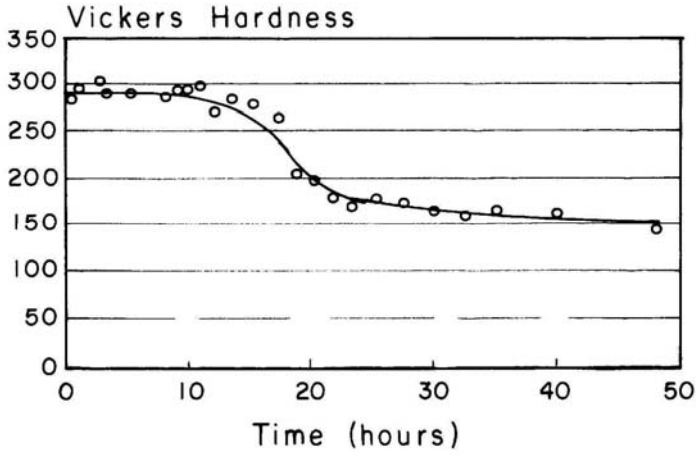

Figure 2: Hardness variation in the samples along the simulated annealing cycle.

Maximum Deviation	22.00
Minimum Deviation	-11.00
Average Deviation	1.86
Standard Deviation	8.04
Mean Standard Error	1.52

Table III: Mean value statistical analysis of the deviations between aimed and real simulated annealing cycle temperatures.

Sample	**Recrystallized Fraction [%]**	**Grain Size [μm]**
O	0.00	---
P	3.73	---
Q	21.58	---
R	28.43	---
S	47.12	---
T	93.25	4.30
U	100.00	4.50
V	---	4.65
W	---	5.00
X	---	5.15
Y	---	5.20
Z	---	5.25
ZA	---	5.60

Table IV: Recrystallized fractions and ferritic grain sizes for the recrystallized samples.

The extracted precipitates were identified through X-ray diffraction as niobium carbides (NbC) through the comparison of the sprectrum peaks with the standard cards of the Joint Committee on Powder Diffraction Standards – J.C.P.P.S.

It was impossible to detect any difference between the totally cold worked **LTF** and recovered **F** samples through transmission electronic microscopy. The start of ferritic recrystallization could be detected in sample **P** because its microstructure exhibited recrystallized and non-recrystallized regions, as shown in figure 5.

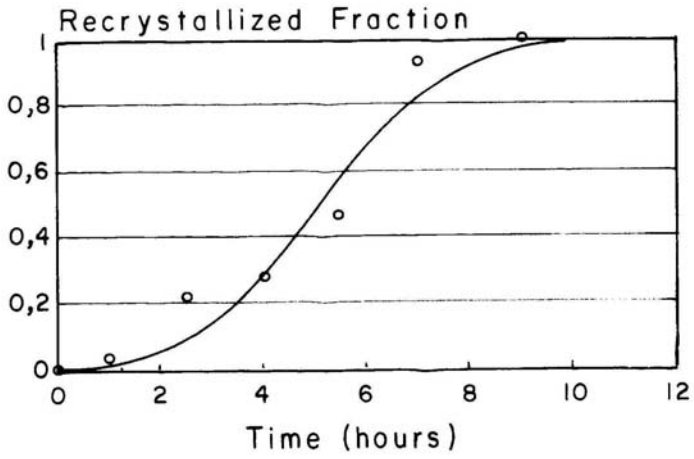

Figure 3: Evolution of the recrystallized fractions after recrystallization start.

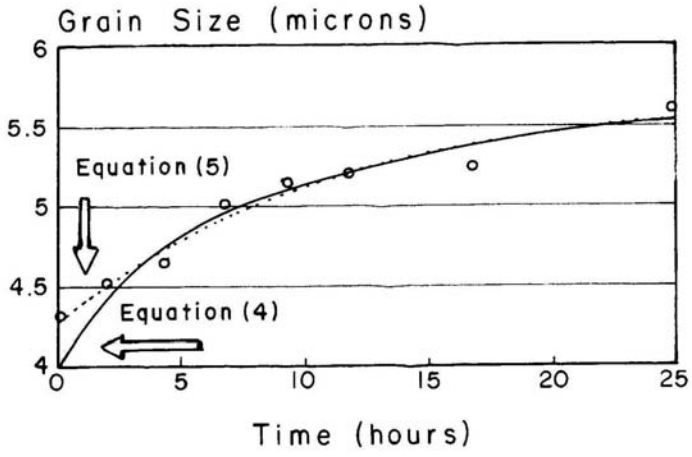

Figure 4: Evolution of the ferritic grain size after complete recrystallization.

Sample **Q** was almost completely recrystallized, as can be seen in figure 6. One can note in this microstructure the presence of fully

recrystallized and not completely recrystallized grains, the latter ones showing heterogeneous grain sizes in the same sample.

The sample **ZA** was completely recrystallized and showed some grain growth, as can be seen in figure 7.

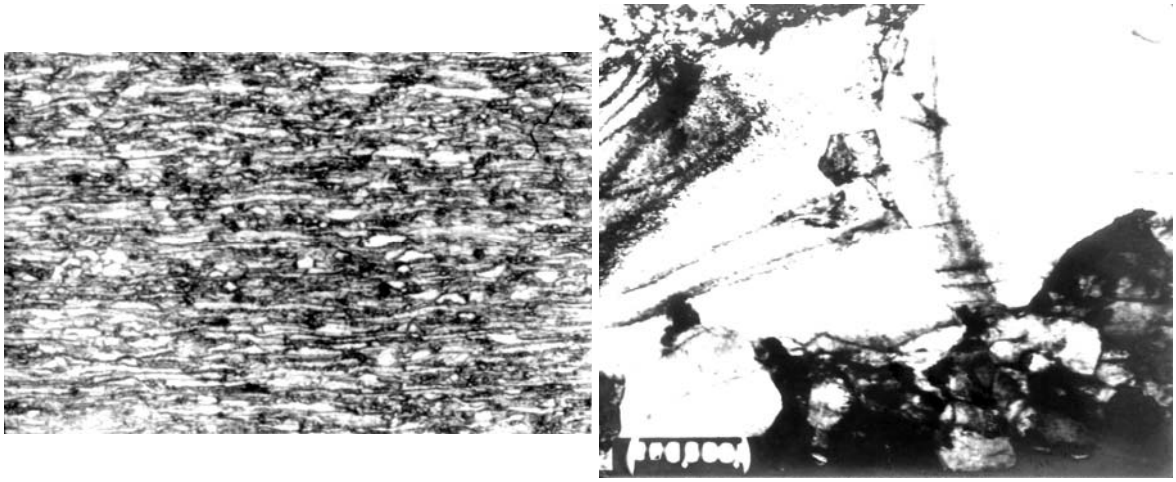

Figure 5: Microstructure of sample **P**, with recrystallized and non-recrystallized regions. Left: optical microscopy, Nital etching, magnification of 500 x. Right: transmission electronic microscopy, magnification of 6,000 x.

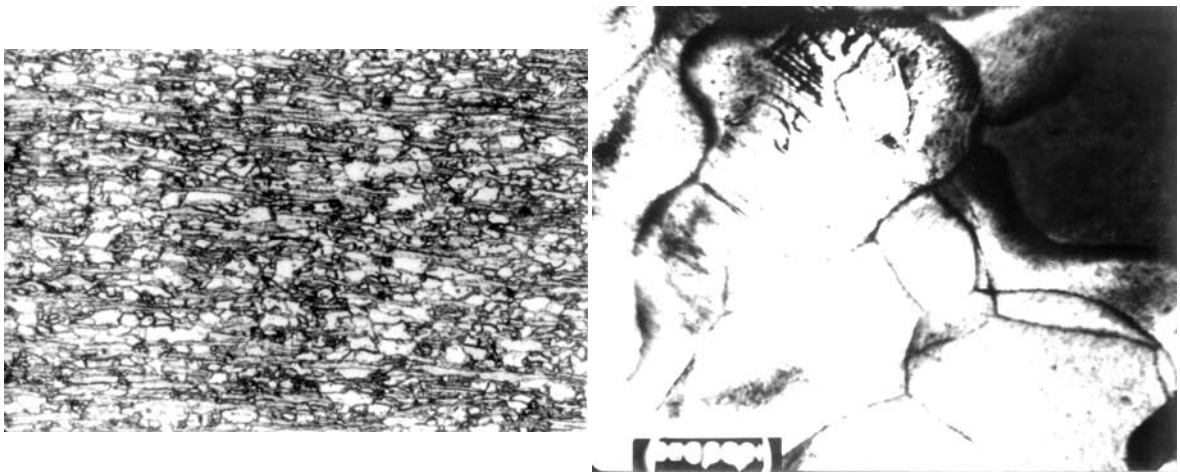

Figure 6: Microstructure of sample **Q**, with grains already recrystallized. Left: optical microscopy, Nital etching, magnification of 500 x. Right: transmission electronic microscopy, magnification of 15,000 x.

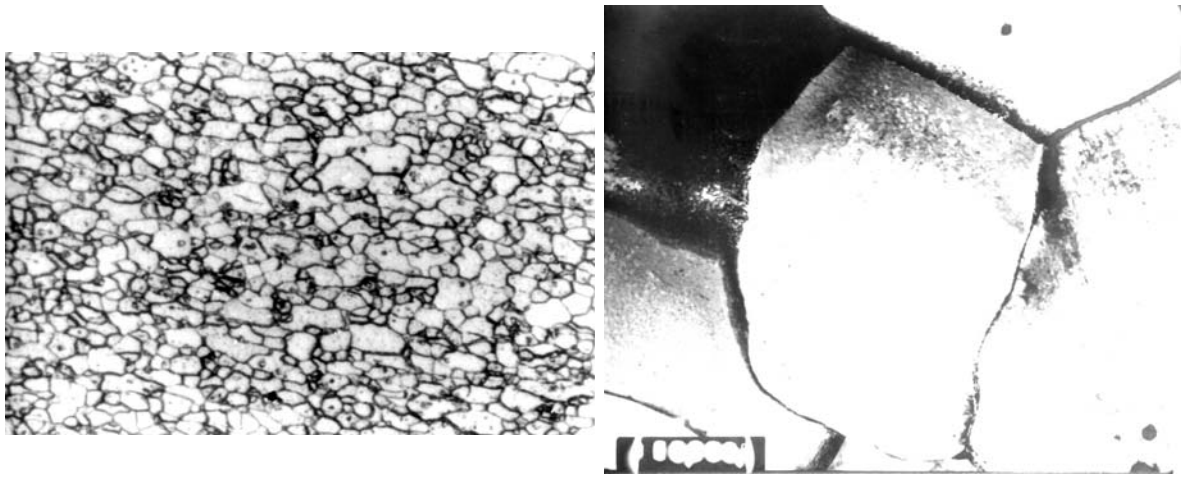

Figure 7: Microstructure of sample **ZA** with recrystallized ferritic grains. Left: optical microscopy, nital etching, magnification of 500 x. Right: transmission electronic microscopy, magnification of 6,000 x.

- DISCUSSION

Table I and figure 2 shows that hardness slightly increased during the first three hours of the simulated annealing cycle; sample **F** showed maximum hardness (303 HV). After that sample hardness remained practically unchanged until the 17th hour of treatment (sample **P**). Probably during this treatment stage a competition between recovery of deformed grains and precipitation of a second phase is taking place. The precipitation could be responsible for the increase in sample hardness (as seen in samples **A** to **F**), until the effects of recovery processes acting in the cold worked material were too intense and promoted its softening (samples **G** to **P**). The precipitated second phase was constituted of Nb carbides, as some amount of this element was solubilized in the ferritic matrix due to the relative low coiling temperature applied to the steel studied – 600°C. These carbides were finely dispersed in ferrite and certainly delayed the recovery process. After the 17th hour of annealing (sample **P**) the hardness sharply decreased and then tended to stabilize (sample **S**). This feature has a relation with the

beginning of ferrite recrystallization, which promoted a rapid hardness decrease of the samples.

Figure 2 also shows that furnace cooling lead to a hardness decrease. Sample **ZA**, submitted to that cooling pattern, showed hardness equal to 140 HV hardness, while sample **Z**, which was rapidly cooled just after the soaking period, showed 160 HV hardness. For its turn, the sample annealed in the plant, **REC**, had hardness equal to 135 HV, very close to the value observed for sample **ZA**. This proves that the laboratory simulated annealing cycle was quite similar to the industrial one; the very low 5 HV difference can be attributed to the ± 5% statistical error associated with the measured hardness values.

It can be seen in figure 8 that recrystallization start temperature was in the range from 600 to 612°C, that is, between the samples **P** (extracted at 606°C) and **Q** (extracted at 612°C), as the hardness difference between these two samples was very significant. It must be remarked that sample **Q** was took off from the furnace 90 minutes after sample **P**.

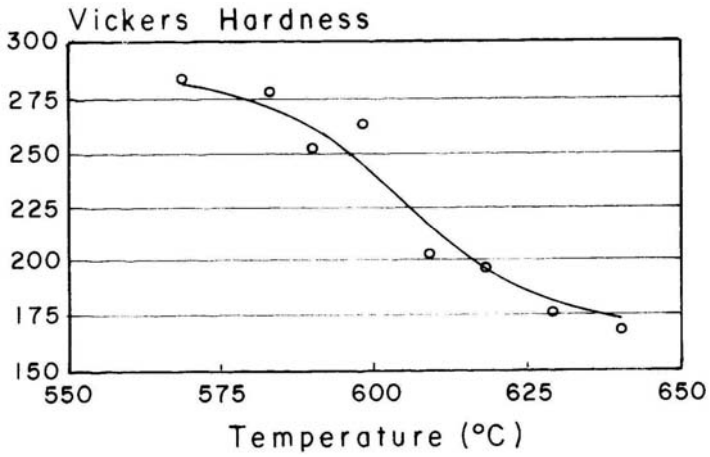

Figure 8: Hardness evolution between the samples from **AA** to **T** versus the real temperature in the moment when each sample was took off.

Table IV and figure 5 show that the beginning of recrystallization can be detected through optical microscopy analysis in sample **P**. Its end can be seen, using the same technique, in sample **U**. These evidences were confirmed by hardness data, which showed that a sharp decrease in this

parameter was verified for the test pieces following the **P** sample due to the recrystallization in progress.

It can be concluded from figure 4 that recrystallization kinetics followed an Avrami-like law:

$$f_r = 1 - \exp(-B\,t^k) \qquad (1)$$

where $\mathbf{f_r}$ is the recrystallized fraction and **t** is time in hours, counted from the start of recrystallization.

The following formula was obtained fitting this equation with data got in this work, using non-linear regression modeling [14]:

$$f_r = 1 - \exp(-0.00566\,t^{2.958}) \qquad r^2 = 0.949 \qquad (2)$$

Formally speaking, the Avrami equation describes kinetics of the isothermal recrystallization [15]. However, the annealing process studied in this process was anisothermal, as it is performed along a determined range of increasing temperatures. However, one can consider this annealing as a sequence of isothermal annealing treatments which actuates each one during a period of time **dt**. The constants **B** and **k** of the equation (2) would be, say, "average" values relative to the correspondent equations for each temperature inside the applied range. However, it must be noted that the value of the constant **k** got in this work, 2.958, is between 2 and 3, which is characteristic for Avrami equations determined for recrystallization treatments in the bidimensional case [15], which is exactly the case of this study. This event could be attributed to the fact that this constant is, as a matter of fact, function of nucleation and growth conditions, while constant **B** effectively changes with temperature [15]. However, it must be stated that equation (2) is valid only for the specific conditions of the annealing process studied in this work.

Figure 4 shows the evolution of the recrystallized ferritic grain size along time after the end of recrystallization, considering samples **U** through

Z. In this case the temperature prevailing along the period of grain growth was practically constant, as the simulated annealing cycle was in the soaking period under a nominal temperature of 670°C. So this case can be considered as being an isothermal grain growth treatment, which can be described by equation (3):

$$D = C\,t^{n} \qquad (3)$$

where **D** is the mean diameter of the ferritic grain in μm; **t** is time in hours, counted from the end or recrystallization; **C** and **n** are constants which are independent from time. The first one strongly depends on temperature, while the other is a function of the alloy being recrystallized, being equal to approximately 0.5 in the case of pure metals. Equation (3) is asymptotic in relation with time, as grain growth stops as a determined critical value is reached; this value depends on temperature [15]. The fitting of grain growth data got in this work through non-linear regression modeling [14] deduced the following equations:

$$D = 4.1965\,t^{0.0870} \qquad r^2 = 0.950 \qquad (4)$$

$$D = 5.7119 - 1.4280 \times 0.91557^{t} \qquad r^2 = 0.970 \qquad (5)$$

It must be noted that both equations (4) and (5) are appropriate to describe asymptotic models. The value of the constant **n** of equation (4) was very low: only 0.0870, comparing with 0.5 got for pure metals. However, this fact can be justified as the steel studied in this work is not, of course, a pure metal, and its grain boundary migration is strongly impaired by the concentration and dispersion degree of Nb carbides, as well by alloy elements present in solid solution. This corresponds mathematically to a decrease in the constant **n** of equation (4).

The grain size of sample **ZA**, that was submitted to the simulated annealing cycle, was equal to 5.6 μm, very near to that measured for the sample **REC**, got from a coil annealed under industrial conditions: 5.2 μm.

The difference observed, 0.4 μm, can be attributed to the statistical dispersion associated to the quantitative metallography measurements.

Figure 9 shows that there is a linear correlation between the hardness and grain size of the ferrite of fully recrystallized samples. The fitted equation is

$$HV = 307 - 29\,D \qquad r^2 = 0.890 \qquad (6)$$

where **HV** is the Vickers hardness and **D** the mean ferritic grain size in μm.

The very close values of hardnesses and grain sizes observed for the samples **ZA** (annealed at the laboratory) and **REC** (annealed at the plant) suggest that the cooling period applied to the coils after batch annealing can be reduced from 54 to 8 hors, without any significant alterations in steel properties. However, it must be noted that operational problems can make this cooling time reduction impossible or, at least, very difficult.

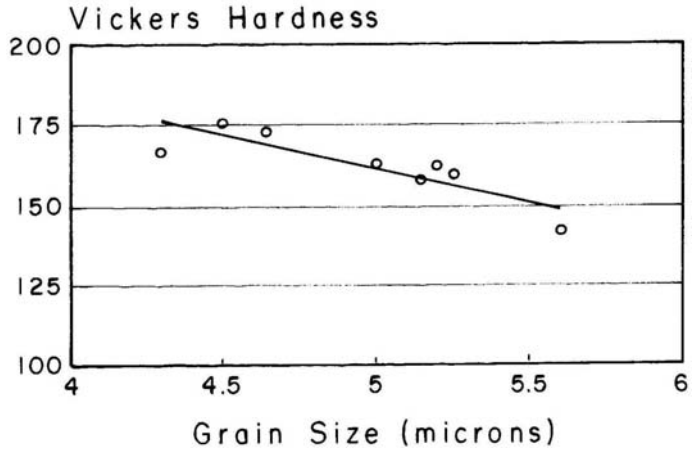

Figure 9: Linear correlation observed between hardness and ferritic grain size of the fully recrystallized samples.

- CONCLUSIONS

The method proposed in this work for the physical simulation of the batch annealing of steel coils in a computer controlled muffle furnace was

very successful, as temperature differences between the proposed and real simulated annealing cycle were very low. The hardness and grain size of the samples processes at the plant and at laboratory were very similar too.

The simulation of a specific batch annealing treatment showed that possibly there is a competition between carbide precipitation and recovery processes up to the 17th hour of treatment or, in this case, up to 610°C. Recrystallization started from this point on, promoting a sharp decrease in the hardness of the samples.

The fitting of theoretical recrystallized fraction and grain size kinetics equations with data got in this work was very good.

Finally, it was verified that the cooling time of the coils after batch annealing can be reduced from 54 to 8 hours without any harm to product properties.

- BIBLIOGRAPHICAL REFERENCES

1. BRANCHINI, O.L.G. & GORNI, A.A. Correlação Matemática entre Temperaturas de Carga em Fornos de Recozimento. In: 43° Congresso Anual da ABM. **Anais**. Belo Horizonte, 1988, 411-423.

2. BRANCHINI, O.L.G. & TSCHIPTSCHIN, A.P. **Simulação Física de Recozimento de Bobinas em Caixa**. Relatório FDTE – Projeto 452, 1989.

3. HOOK, R.E. et al. Recrystallization of Deep Drawing Cb (Nb)-Treated IF Sheets Steels. **Metallurgical Transactions A**, 6:7A, July 1975, 1443-1451.

4. GAVEN, J.A. et al. Observation of the Recrystallization Mechanism in the Ferrite in Some C Steels Containing Small Additions of Alloy Elements. **Scandinavian Journal of Metallurgy**, 4, 1975, 250-254.

5. GLADMAN, T. Effect of Carbide and Nitride Particles on the Recrystallization of Ferrite. **Journal of the Iron and Steel Institute**, May 1971, 380-90.

6. MESSIEN, P. et al. Recrystallization and Plastic Anisotropy of Low C-Ti and Nb Steels. **C.R.M. Metallurgical Reports**, Dec. 1976, 3-21.

7. SATOH, S. et al. Effect of Precipitate Dispersion on Recrystallization Texture of Nb Steel Sheet. **Transactions of the ISIJ**, 1986, 737-44.

8. MOULD, P.R. et al. Plastic Anisotropy of Low C, Low Mn Steels Containing Nb. Metallurgical Transactions, 3:12, Dec. 1972, 3121-3132.

9. DAVIDSON, A.P. et al. Structural and Textural Aspects of Deformation and Recrystallization of Low C Steels Containing Dispersions of Nb(CN). Metal Science, March-April 1979, 170-178.

10. PADILHA, A.F. & AMBRÓSION FILHO, F. **Técnicas de Análise Microestrutural**, Editora Hemus, São Paulo, 1985, 190 p.

11. ASTM. Determining Volume Fraction by Systematic Manual Point Count. **A.S.T.M. Standard E 562-76**, 1982.

12. ASTM. Estimating the Average Grain Size of Metals. **A.S.T.M. Standard E 112-76**, 1982.

13. ASTM. Microhardness of Materials. **A.S.T.M. Standard E 184-76**, 1982.

14. RATKOWSKY, D.A. **Non-Linear Regression Modelling**. Marcel Dekker, New York, 1983, 252 p.

15. GORELIK, S.S. **Recrystallization in Metals and Alloys**. MIR Publishers, Moscow, 1981, 479 p.